U.P.B. Sci. Bull., Series C, Vol. 81, Iss. 2, 2019 ISSN 2286-3540

NEW ANALYTICAL FORMULAS FOR SELF-INDUCTANCES OF INDUCTIVELY COUPLED RING COILS IN WIRELESS POWER TRANSFER SYSTEM

Mohammed AL-SAADI*[1], Sadiq AHMED[2]
Ammar IBRAHIM[2], Mustafa AL-QAISI[2], Aurelian CRĂCIUNESCU[1]

In this paper, using response surface methodology, the analytical relationships as functional dependencies on the 7 specified geometrical parameters are established for self-inductances of an inductive power transfer (IPT) device. Using the variance analysis, the sensitivity of the self-inductance values to variations in the geometric parameters of the IPT device was studied. The established analytical relationships allow for easy determination of the self-inductance values specific to the IPT devices for their different geometric configurations, including for different misalignments. They are also particularly useful in optimal design of the IPT devices.

Keywords: wireless power transfer, wireless charging, inductively coupled coils, self-inductance, Box-Behnken design, response surface methodology

1. Introduction

The wireless power transfer (WPT) technology has a pivotal role in the vastly spreading of the contactless charging, for electric vehicles (EVs), E-book readers, smartphones, biomedical devices, digital camera and laptops etc [1]. This technology is convenient and safer than the wire one. The WPT for the batteries charging includes two non-radiative (near field) technologies: inductive power transfer (IPT) based on the time-varying magnetic field, and capacitive power transfer (CPT) based on the time-varying electric field [2-6]. In this work, only IPT technology investigated. This technology based on the Ampère's law, when one of the coils is excited with a time-varying current, it generates a time-varying magnetic field. If this field traverses another coil, a voltage difference is induced between its terminals [7].

Broadly, a coil can take many shapes, such as ring, rectangular, square, etc. It has been found that the coils shapes and theirs physical parameters have a considerable effect on its power capability, power transfer distance (air-gap), and misalignment behaviour [7]. Much studies over the past few years, have been

---

[1] Electrical Engineering Faculty, University POLITEHNICA of Bucharest, Bucharest, Romania. *Correspondent author. E-mail: mohamedshihab91@gmail.com
[2] Engineering Faculty, Electrical Engineering Department, AL-MUSTANSIRIYAH University, Baghdad, Iraq

concentrated on the improving the IPT capability in terms of optimization their physical coils parameters [8] [9]. The self-inductances of the transmitter (L_1) and receiver (L_2) coils have a big influence on the power factor and energy transfer capability of an IPT system. The reactive inductive power is consumed by the L_1 and L_2, which result in an increasing the VA ratings of the components, power factor reducing, and losses [10]. Therefore, optimizing the L_1 and L_2 parameters, the system performances can be optimized.

One way to enhance the IPT system performances is to use a capacitor(s) connected in series/parallel with transmitter and receiver coils to compensate the reactive power; this is so called resonance technology; it was proposed by MIT in 2007 [1]. For purpose of completely compensating the inductive reactive power, it is necessary to know the L_1 and L_2 values. The L_1 and L_2 are usually numerical calculated, after the coils have been designed, by using the finite element analysis (FEA) or, with analytical formulas, by utilizing volume integrals derived from the magnetic energy expression, as described in [11], [12]. On the other hand, J. Sallan et al. carried out calculations to introduce analytical formulas for the L_1 and L_2 of the inductively coupled rectangular and planar coils configurations using Neumann's expression. The introduced formulas are just function of the geometrical parameters [13].

In this paper, the response surface methodology (RSM) is used as a tool to obtain new analytical formulas of L_1 and L_2 for purpose of the optimization and facilitating the design of the inductively coupled two ring coils. On the basis of this approach, with these formulas, analytical relationships will be established between the self-inductances and their corresponding geometrical parameters i.e. coils dimensions, air-gap, and misalignments; a ferrite plate behind each coil is considered. The analytical formulas for the L_1, and L_2 can be used in the IPT system for optimal design. This is a novel step for optimization the inductively coupled ring coil parameters.

This paper is arranged as follows: section 2 describes the fundamentals of the IPT system. Section 3 presents the proposed methodology of introducing analytical formulas for L_1 and L_2. Section 4 shows the simulation outcomes and discussion. Section 5 validates the introduced formulas of the L_1 and L_2 with the FEA calculation results. Finally, section 6 formulates appropriate conclusions.

2. Fundamentals of the inductive power transfer system

2.1. Typical system structure

An IPT typical system structure for contactless power transfer is shown in Fig. 1. It is consisting of a transmitter side and a receiver side. The transmitter side includes the following components: a rectifier; an inverter which is used to excite the transmitter coil with a high AC voltage at high frequency, and a compensation circuit to create an electric field in resonance. The receiver side components are the following: a receiver coil which function is to pick up the electromagnetic field from the transmitter coil, and a rectifier which function is to supply the load with a DC output voltage (V_L) [7]. The purpose of the compensation circuits in the transmitter and receiver sides is to create an electric field in resonance.

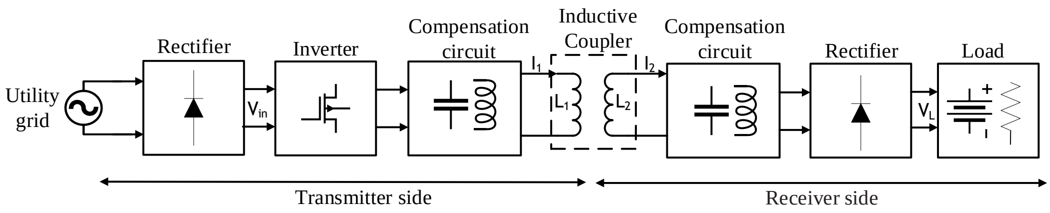

Fig. 1. Typical system structure of an IPT

The parameters that used to describe the inductively coupled coils are: L_1, L_2, the mutual inductance (M) and coupling coefficient (k). The relation between these parameters are expressed by equation (1).

$$M = k\sqrt{L_1 L_2} \tag{1}$$

In a series-series (SS) compensated IPT system, at resonance, the power (P_L) delivered to the load (R_L) is expressed by equation (2); (the internal resistances of the coils are neglected) [1].

$$P_L = \frac{\omega^2 I_1^2 M^2}{R_L} = \frac{\omega^2 I_1^2 k^2 L_1 L_2}{R_L} \tag{2}$$

2.2. Coil configurations

In this paper, the ring configuration was chosen to represent the inductively coupled coils. A ferrite plate of disc configuration, as it is shown in Fig. 2a, is usually used behind each coil to enhance k [14]. The physical design parameters of the inductively coupled ring coils are: the outer radius (r_2) and the inner radius (r_1) of the transmitter coil; the outer radius (R_2) and inner radius (R_1) of receiver coil; the air-gap (d) between inductively coupled coils (Fig. 2b). The difference between the outer and inner radii represent the equivalent radius of the windings.

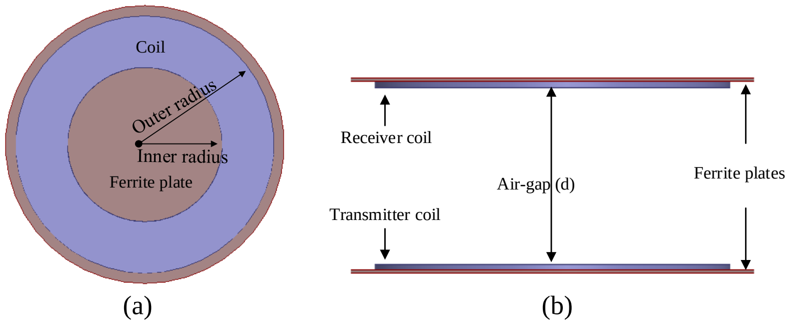

Fig. 2. (a) A ring coil with ferrite plate, (b) Well aligned inductively coupled coils.

2.3. Misalignment

The misalignment is the deviation of the receiver coil from its normal position with respect to the transmitter coil. However, the considered misalignments cases are: lateral misalignment (L) and angular misalignment (α) (Fig. 3a and 3b).

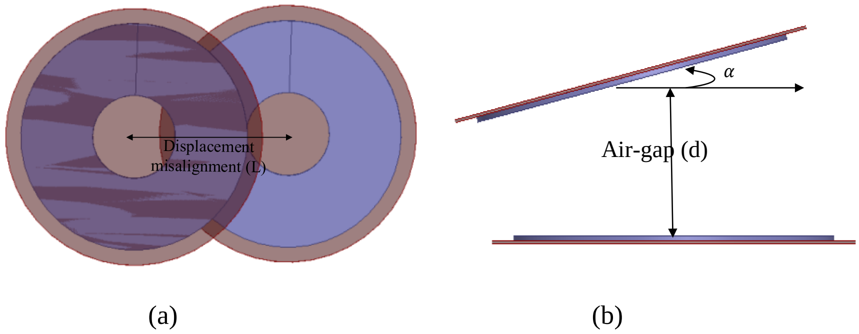

Fig. 3. (a) Lateral misalignment (b) Angular misalignment.

3. Methodology

This study involves the analyzing of inductively coupled two ring coils to determine analytical formulas for their self-inductances i.e. L_1, and L_2. The values of these inductances are tested as a function of the geometrical parameters i.e. physical parameters of the coil, the airgap and misalignment parameters. Electromagnetic field finite element analysis (FEA) and response surface analysis (RSA) were used to obtain the L_1 and L_2 analytical models.

Firstly, several FEA simulation were conducted in the ANSYS Maxwell software to determine the L_1 and L_2 for the various geometrical parameters according to the requirements of the RSA. Secondly, the FEA outcomes were inserted into JMP software to conduct the RSA.

3.1. Finite element analysis

The IPT system consists of two ring coils of Litz copper wire; these coils are geometrically similar, but their physical dimensions may be different. Each coil is mounted on a ferrite plate with a radius of 4 cm bigger than the outer radius of the respective coil, as it is shown in Fig. 2a. The skin effect is not considered, since the coils are wound utilizing Litz wire. However, the FEA was implemented with the aid of the ANSYS Maxwell version 16.

3.2. Response surface analysis

The RSA utilizes the quantitative analysis data from a relevant experiment to build the regression model of a parameter and to find the optimal value of this parameter which is dependent on several others parameters, by using minimum number of experimental data [15].

In this work, a quadratic surface fitting model is used to obtain information on the dependences of the L_1 and L_2 on their geometrical parameters. The so-called experimental data needed to construct the response surfaces were obtained by electromagnetic field calculations which made using the ANSYS Maxwell software version 16.

The obtaining of an analytical model with RSA presumes the followings three major steps [15], [16]:

a) a multivariate design of experiment (DOE);

b) a design technique applied to estimate the coefficients that represent the effect level of each parameter on the output model. In this study, the Box-Behnken design technique was applied to calculate the linear, quadratic and mixed parameter interactions influences on the output model parameter.

c) analysis of variance (ANOVA) which is applied to evaluate the output of the quadratic model; further, the ANOVA screening the fit degree of the actual model with the output predicted model. In this study, the RSA was accomplished with the help of the JMP statistical software.

3.2.1. Multivariate design of experiment (DOE)

The multivariate DOE, based on the RSA, was implemented with the following considerations: The L_1, and L_2 are the output responses; the r_1, r_2, R_1, R_2, d, L, and α are the input independent parameters. In our study, these seven geometrical design and misalignment parameters are varied with their ranges which are listed in Table 1. These ranges are usually used in the EVs charging applications. However, the minimum, maximum, and medium parameters range levels are coded in the JMP software as -, +, and 0, respectively.

Table 1

The ranges of the ring coil dimensions and misalignments in an IPT system.

Studied points	r_1 (cm)	r_2 (cm)	R_1 (cm)	R_2 (cm)	d (cm)	L (cm)	α (deg)
Minimum	2	30	2	30	10	0	0
Maximum	20	60	20	60	50	20	7
Medium	11	45	11	45	30	10	3.5

3.2.2. Design techniques

Based on the Box-Behnken design methodology, a total of 62 simulated data are required for seven geometrical parameters [15] (i.e. four design parameters, air-gap, and two misalignment parameters), where in each simulation one/more parameter(s) varied regularly between their maximum, minimum and medium values. The data were obtained using the FEA ANSYS Maxwell software which then have been inserted into JMP software to implement the RSA. The effect level of each parameter on the L_1, and L_2 was measured.

In the statistical analysis, the input variables with their corresponding response were modelled to optimize the process conditions for the required response. The ANOVA is used to determine the statistical parameters with the aid of Box-Behnken design [16].

3.2.3. Analysis of variance (ANOVA)

The ANOVA has been implemented by using the JMP statistical software for the regression analysis. In the same software, the significance of the statistical analysis was examined. The parameter R^2 is indication of the degree of the model fit. The significance level of each term in the polynomial model was evaluated by the F-value or probability value (P-value) at 95% confidence interval [15].

The ANOVA table which result from the RSA contains the following columns: source, degree of freedom (DF), sum of squares, mean square, F-value, and P-value. The F-value and P-value are necessary to evaluate the response surface of a model. The significance factor is described by F-value or P-value with a 95% of confidence level. This means only the terms of P-value less than 5% or 0.05 are significant. The large F-value (or the small P-value) of a term indicates its significant effect on the output response [15].

4. Results and discussion

In this section, novel formulas for L_1 and L_2 of Litz copper wire for ring coils are obtained. Each one of these parameters was tested as a function of seven design and misalignment parameters with their ranges, as were mentioned earlier in section 3.2.1. Based on the Box-Behnken design, a total of 62 simulation data are required for the seven variable parameters [15]. In our study, these data were obtained using FEA in ANSYS Maxwell software, then inserted into JMP software, as listed in Table 2.

Table 2

Box–Behnken design of two output responses as function of seven input variables

No.	Pattern	Independent input variables							Output responses due FEA	
		r_1 (cm)	r_2 (cm)	R_1 (cm)	R_2 (cm)	d (cm)	L (cm)	α (deg)	L_1 (μH/turns^2)	L_2 (μH/turns^2)
1	− −0−000	2	30	11	30	30	10	3.5	0.41939	0.75919
2	− −0+000	2	30	11	60	30	10	3.5	0.42282	1.044
3	−0−000−	2	45	2	45	30	10	0	0.61233	0.61188
4	−0−000+	2	45	2	45	30	10	7	0.61096	0.61449
⋮	⋮	⋮	⋮	⋮	⋮	⋮	⋮	⋮	⋮	⋮
61	+0+000+	20	45	20	45	30	10	7	1.3438	1.3456
62	++0−000	20	60	11	30	30	10	3.5	1.4183	0.76917

The effect of the ferrite plates on the parameters of the inductively coupled coils was tested under these considerations: r_1= R_1=10cm, d=10cm, r_2=R_2=30cm, and number of turns in the primary (N_1) and secondary (N_2) coils are 26. Firstly, with the existence of ferrite plates the FEA outcomes are: L_1=561.23μH, L_2=561.88μH, M=330.89μH, k=0.589. Secondly, under same consideration but with the absence of the ferrite plates the parameters are: L_1=289.53μH, L_2=278.38μH, M=116.3μH, k=0.409. Based on these outcomes, L_1, L_2, and M are reduced to approximately half of their values with the absence of the ferrite plates. According to equation (2), the M has the highest effect on the load power than the self-inductances of the transmitter and receiver coils.

4.1. Development the model of the transmitter self-inductance (L_1)

4.1.1. ANOVA of the L_1 model

The ANOVA table of the reduced quadratic L_1 model is presented in Table 3 (terms that have P-value greater than 0.05 were removed). For this reduced model, the F-value in Table 3 is as many as 542.5, and the lack-of-fit is significant due to its F-value>0.05. This refers that this model is considered to be statistically significant. The following individual parameters r_1, r_2, R_2, and d, and interaction parameters, r_1*r_2, r_1*d, r_2*d, R_2*d, r_1*r_1, and d*d, are considered significate terms in the L_1 model, since their P-values less than 0.05.

According to the F-values from the Table 3, the r_1 has the most considerable impact on the L_1. The only quadratic term of r_1, and d, have an effect on L_1. On the other hand, the α, and L have a negligible effect on L_1. This signifies that only the design parameters have a significant effect on the L_1. Hence, only the parameters and terms that have a significant effect on L_1 are appear in the L_1 model which can be described by equation (3).

Table 3

ANOVA for the L_1 model after eliminations of the insignificant terms.

Source	**DF**	**Sum of Squares**	**F Ratio**	**Prob > F**
Model	10	5.0080928	542.5044	
r_1	1	3.6298604	3932.066	<.0001*
r_2	1	0.5832032	631.7581	<.0001*
R_2	1	0.0190159	20.5991	<.0001*
d	1	0.4428167	479.6836	<.0001*
r_1 *r_2	1	0.0327910	35.5211	<.0001*
r_1 *d	1	0.0221299	23.9723	<.0001*
r_2 *d	1	0.0130153	14.0989	0.0004*
R_2 *d	1	0.0237075	25.6813	<.0001*
r_1 *r_1	1	0.0879142	95.2336	<.0001*
d *d	1	0.1734437	187.8839	<.0001*
Error	51	0.0470803		
Lack of fit	16	0.04074961	14.0806	
Pure error	35	0.00633069		
Correlated total	61	5.0551731		

This equation can be multiplied by the square of the number of turns in the primary coil (N_1^2) to get the primary self-inductance in (μH).

$$L_1(\mu H/turns^2) = 0.91493855 + 0.388901.\left(\frac{r_1 - 11}{9}\right) + 0.155885.\left(\frac{r_2 - 45}{15}\right) + 0.02814833.\left(\frac{R_2 - 45}{15}\right) - 0.1358333.\left(\frac{d - 30}{20}\right) - 0.0640225.\left(\frac{r_1 - 11}{9}\right).\left(\frac{r_2 - 45}{15}\right) - 0.052595.\left(\frac{r_1 - 11}{9}\right).\left(\frac{d - 30}{20}\right) - 0.040335.\left(\frac{r_2 - 45}{15}\right).\left(\frac{d - 30}{20}\right) - 0.0544375.\left(\frac{R_2 - 45}{15}\right).\left(\frac{d - 30}{20}\right) + 0.0776078.\left(\frac{r_1 - 11}{9}\right)^2 + 0.1090071755.\left(\frac{d - 30}{20}\right)^2 \quad (3)$$

For a good model, standard deviation (SD) is desired to be low and R^2 near unity [17], [16]. For the L_1 model, the SD is only 0.2878744 with R^2 as many as 0.99.

4.1.2. Effect of the input parameters on L_1 model

Fig. 4 shows the L_1 behavior according to equations (3). The parameters are arranged depending on their significant effect level on the L_1.

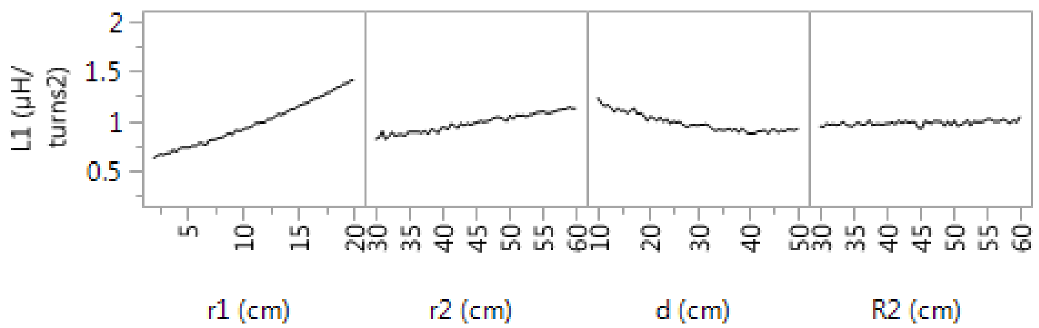

Fig. 4. Effect of the design parameters of the transmitter coil on L_1.

As can be observed from Fig. 4, the L_1 is considerably increasing as r_1 increases. Likewise, as the r_2 increases the L_1 slightly increases. However, the increasing of r_1 or r_2 has as result the increase of the L_1 value. On the other hand, the d has a slight effect on L_1. The L_1 is insensitive to R_2 variation.

The numerical representation was applied, to measure the percentage effect level of the design parameters on L_1. The r_1 has the most significant effect on L_1 which is 76%. The r_2 and d have almost the same effect which is only of 12% and 11%, respectively. The R_2 has a negligible effect of barely 1%. However, the 3D plot of the r_1 and r_2 effect on the L_1 is illustrated in Fig. 5. As can be seen from Fig. 5, the maximum value of L_1 occurs at only maximum r_1 and over wide range of r_2.

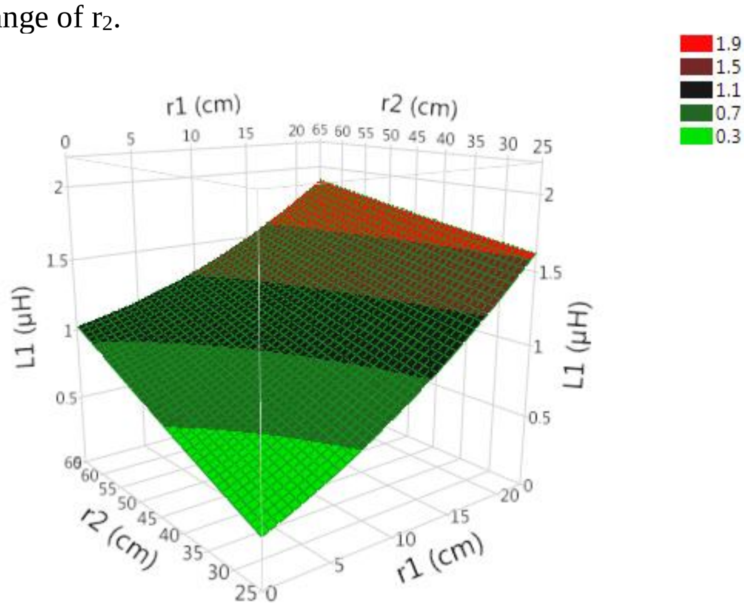

Fig. 5. Effect of the r_1 and r_2 on the L_1 at d=15cm, and R_2=45cm.

4.2. Development the model of the receiver self-inductance (L_2)

4.2.1. ANOVA of the L_2 model

The terms that have P-value greater than 0.05 were removed from ANOVA table of L_2 model because of their negligible effects. The ANOVA table of the reduced L_2 quadratic model is listed in Table 4. For this reduced model, the F-value is as many as 341.8838, and the lack-of-fit is significant due to its F-value> 0.05. This indicates that this model is considered to be statistically significant. The following individual parameters r_2, R_1, R_2, and d, and interaction parameters, r_2*R_1, R_1*R_2, r_2*d, R_1*d, R_1*R_1, and d*d, are considered significate terms in the L_2 model, since their P-values less than 0.05.

Table 4

ANOVA for the L_2 model after eliminations of the insignificant terms.

Source	DF	Sum of Squares	F-value	Prob > F
Model	10	4.8626185	341.8838	
r_2	1	0.0427418	30.0512	<.0001*
R_1	1	3.4554918	2429.507	<.0001*
R_2	1	0.5565895	391.3301	<.0001*
d	1	0.5029541	353.6199	<.0001*
r_2 *R_1	1	0.0205477	14.4468	0.0004*
R_1 *R_2	1	0.0327680	23.0387	<.0001*
r_2 *d	1	0.0166404	11.6996	0.0012*
R_1 *d	1	0.0389149	27.3605	<.0001*
R_1 *R_1	1	0.0536738	37.7373	<.0001*
d *d	1	0.1568876	110.3054	<.0001*
Error	51	0.0725374		
Lack of fit	16	0.06964437	52.6602	
Pure error	35	0.00289302		
Correlated total	61	4.9451559		

According to F-value column from Table 4, the R_1 has the most significant impact on L_2, the only quadratic term of R_1, and d, have an effect on L_2; the α, L, and r_1 have a negligible effect on L_2. This means that only the design parameters have a significant effect on the L_2. However, only the parameters and terms that have a significant effect are appear in the L_2 quadratic model which can be expressed by equation (4). This equation can be multiplied by the square of the number of turns in the secondary coil (N_2^2) to get the secondary self-inductance in (μH).

$$L_2(\mu H/turns^2) = 0.9226735 + 0.04220083.\left(\frac{r_2-45}{15}\right) + 0.3794454.\left(\frac{R_1-11}{9}\right) + 0.1522866.\left(\frac{R_2-45}{15}\right) - 0.14476333.\left(\frac{d-30}{20}\right) + 0.05068.\left(\frac{r_2-45}{15}\right).\left(\frac{R_1-11}{9}\right) - 0.064.\left(\frac{R_1-11}{9}\right).\left(\frac{R_2-45}{15}\right) - 0.0456075.\left(\frac{r_2-45}{15}\right).\left(\frac{d-30}{20}\right) - 0.069745.\left(\frac{R_1-11}{9}\right).\left(\frac{d-30}{20}\right) + 0.06063967.\left(\frac{R_1-11}{9}\right)^2 + 0.103674.\left(\frac{d-30}{20}\right)^2 \quad (4)$$

The SD of the L_2 model is only 0.2844366 with R_2 as many as 0.99; this means a good fit model obtained.

4.2.2. Effect of the input parameters on L_2 model

Based on equations (4), Fig. 6 shows the behavior of L_2 due to the design parameters variation. The parameters are arranged depending on their significant effect level.

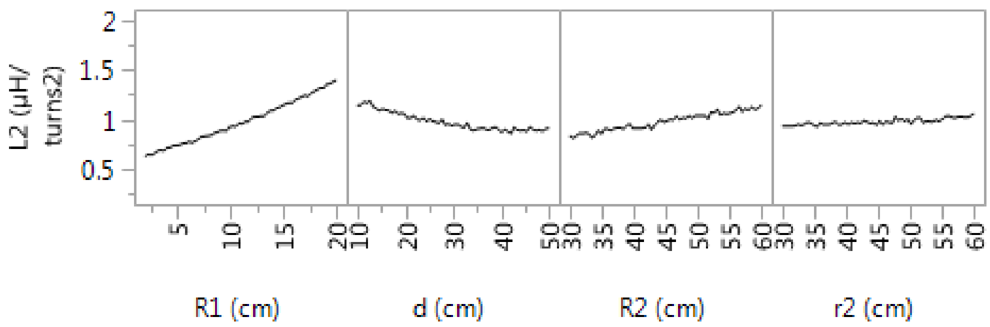

Fig. 6. Effect of the design parameters of the receiver coil on L_2.

As can be observed from Fig. 6, the L_2 is considerably increasing as R_1 increases. Likewise, as the R_2 increases the L_2 is slightly increases. However, the increasing of R_1 or R_2 result in increasing of L_2 value. On the other hand, the d increasing result in slightly decreasing of L_2. The L_2 is insensitive to r_2 variation. However, the numerical representation was applied, to measure the percentage significant effect level of the design and misalignment parameters on L_2. The R_1 has the most significant effect on L_2 which is 75%, the R_2 and d have the same effect i.e. 12%. The r_2 has a negligible effect of barely 1%.

The 3D plot of the R_1 and R_2 effect on the L_2 is depicted in Fig. 7; as can be noted the maximum value of L_2 occurs only at maximum R_1 and over wide range of R_2.

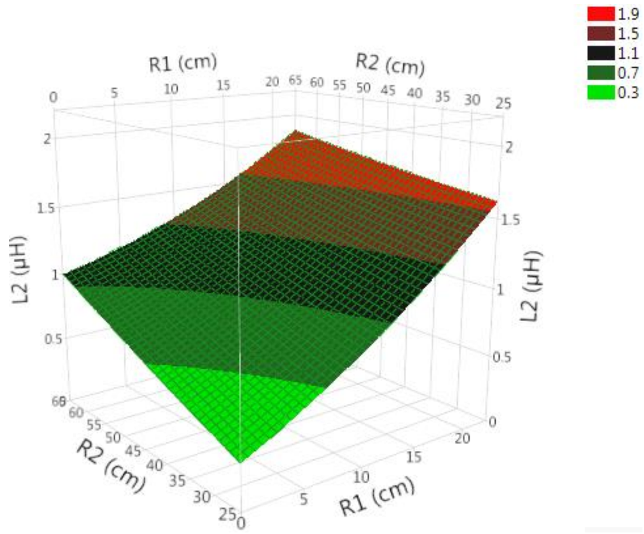

Fig. 7. Effect of the R_1 and R_2 on the L_2 at d=15cm, r_2=45cm.

5. Validation of the L_1 and L_2 models

To verify the analytical formulas of L_1, and L_2, they will be compared with the results obtained with FEA data. Since r_1 has the highest impact on L_1 among all other parameters, it was chosen as a variable parameter to verify the validity of L_1 formula with the following constant parameters: r_2= R_2=30cm, R_1=10cm, d=10cm, and N_1=26 turns. The L_1 results obtained with the presented formula and FEA simulation results are shown in Fig. 8a. In a similar way, since R_1 has the highest impact on L_2 among all other parameters, it was chosen as a variable parameter to verify the validity of L_2 formula with the following parameters: R_2= r_2=30cm, r_1=10cm, d=10cm, N_2=26 turns.

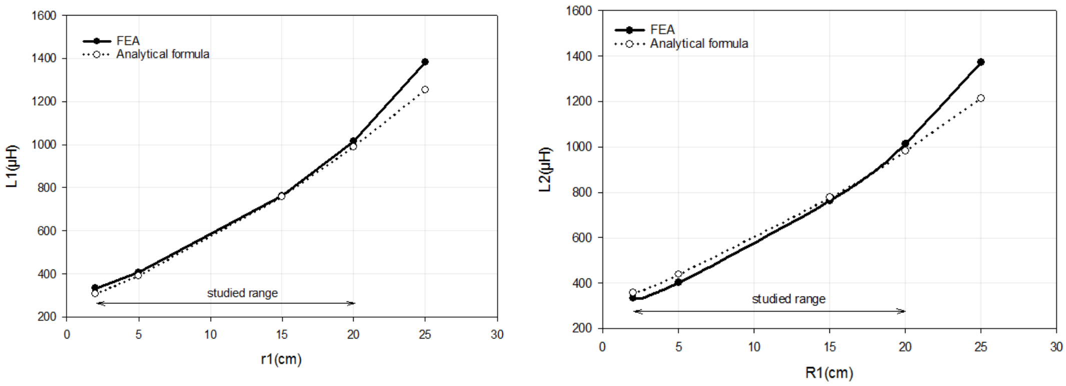

(a) (b)

Fig. 8. Validation of analytical formulas with FEA simulation results (a) L_1 (b) L_2.

The L_2 results obtained with the presented formula and FEA simulation results are shown in Fig. 8b.

As can be seen from Fig. 8a and 8b, the results obtained due to the analytical formulas of L_1 and L_2 agree with the FEA simulation results. This indicates that the introduced formulas of L_1 and L_2 have a very good accuracy within the studied range of the parameters and can be considered during the design of the inductively coupled ring coils. However, the error level of the introduced analytical formulas increases as the input parameters get far from their studied ranges.

6. Conclusions

The advantages of the introduced analytical formulas over the FEA, the analytical formulas are could be calculate the L_1 and L_2 before the coil design. Furthermore, the presented formulas are building a mathematical relationship between the output responses (i.e. L_1 and L_2) as function of the geometrical parameters of the inductively coupled coils.

The percentage effect of each geometrical parameter on the L_1, and L_2 was measured. This measuring has a significant importance in an IPT system design and optimization; which facilitates to specify which parameter has carefully to be designed or has a priority to be optimized. We found out that the self-inductance of a ring coil is most sensitive to its inner radius. Also, the coils parameters (i.e. L_1, and L_2) are insensitive to the misalignment.

The results due to the obtained formulas were consistent with the FEA simulation results. This is compelling evidence that the obtained formulas are applicable for any ring coil in an IPT. However, some restrictions are worth noting. The obtained formulas have a very good accuracy within specified ranges of input parameters which are listed in Table 1. The formulas are still working outside these ranges but the error increases gradually as the input parameters get far from their studied ranges.

R E F E R E N C E S

[1]. Mohammed AL-SAADI, Ali AL-OMARI, Sarab AL-CHLAIHAWI, Ammar AL-GIZI, and Aurelian CRĂCIUNESCU, "Inductive Power Transfer for Charging the Electric Vehicle Batteries," EEA, no. 4, 2018.

[2]. Mohammed AL-SAADI, Ammar AL-GIZI, Sadiq AHMED, Sarab AL-CHLAIHAWI, and Aurelian CRĂCIUNESCU, "Analysis of Charge Plate Configurations in Unipolar Capacitive Power Transfer System for Charging the Electric Vehicles Batteries," in 12th International Conference on Interdisciplinarity in Engineering, 2018.

[3]. Mohammed AL-SAADI, Mustafa AL-QAISI, Layth AL-BAHRANI, and Ali AL-OMARI, and Aurelian CRĂCIUNESCU, "A Comparative Study of Capacitive Couplers in Wireless Power Transfer," in International Symposium on Fundamentals of Electrical Engineering (ISFEE), 2018.

[4]. Mohammed AL-SAADI, Layth AL-BAHRANI, Mustafa AL-QAISI, Sarab AL-CHLAIHAWI, and Aurelian CRĂCIUNESCU, "Capacitive Power Transfer for Wireless Batteries Charging.," Electroteh. Electron. Autom., vol. 66, no. 4, 2018.

[5]. Mohammed AL-SAADI, Emad A. Hussien, Sadiq AHMED, and Aurelian CRĂCIUNESCU, "Comparative Study of Compensation Circuit Topologies in 6.6kW Capacitive Power Transfer System," in THE 11th INTERNATIONAL SYMPOSIUM ON ADVANCED TOPICS IN ELECTRICAL ENGINEERING (ATEE), 2019. (pending publication)

[6]. Mohammed AL-SAADI, Sarab AL-CHLAIHAWI, Mustafa AL-QAISI, and Aurelian CRĂCIUNESCU, "A New Analytical Formula for Coupling Capacitance of Unipolar Capacitive Coupler in Wireless Power Transfer System," in THE 11th INTERNATIONAL SYMPOSIUM ON ADVANCED TOPICS IN ELECTRICAL ENGINEERING (ATEE), 2019. (pending publication)

[7]. Mohammed AL-SAADI, Ammar IBRAHIM, Ali AL-OMARI, Ammar AL-GIZI, and Aurelian CRĂCIUNESCU, "Analysis and Comparison of Resonance Topologies in 6.6kW Wireless Inductive Charging for Electric Vehicles Batteries," in 12th International Conference on Interdisciplinarity in Engineering, 2018.

[8]. J. L. Villa, J. Sallán, A. Llombart, and J. F. Sanz, "Design of a high frequency Inductively Coupled Power Transfer system for electric vehicle battery charge," Appl. Energy, vol. 86, no. 3, pp. 355–363, 2009.

[9]. H. Takanashi, Y. Sato, Y. Kaneko, S. Abe, and T. Yasuda, "A large air gap 3 kW wireless power transfer system for electric vehicles," 2012 IEEE Energy Convers. Congr. Expo. ECCE 2012, pp. 269–274, 2012.

[10]. J. L. Villa, J. Sallán, J. Francisco, S. Osorio, and A. Llombart, "High-Misalignment Tolerant Compensation Topology For ICPT Systems," vol. 59, no. 2, pp. 945–951, 2012.

[11]. S. Babic, S. Salon, and C. Akyel, "The mutual inductance of two thin coaxial disk coils in air," IEEE Trans. Magn., vol. 40, no. 2 II, pp. 822–825, 2004.

[12]. Z. Luo and X. Wei, "Analysis of Square and Circular Planar Spiral Coils in Wireless Power Transfer System for Electric Vehicles," IEEE Trans. Ind. Electron., vol. 65, no. 1, pp. 331–341, 2018.

[13]. J. Sallan, J. L. Villa, A. Llombart, and J. F. Sanz, "Optimal Design of ICPT Systems Applied to Electric Vehicle Battery Charge," IEEE Trans. Ind. Electron., vol. 56, no. 6, pp. 2140–2149, 2009.

[14]. J. Shin et al., "Design and Implementation of Shaped Magnetic Resonance Based Wireless Power Transfer System for Roadway-Powered Moving Electric Vehicles," IEEE Trans. Ind. Electron., vol. 61, no. 3, pp. 1179–1192, 2014.

[15]. D. C. Montgomery, Design and Analysis of Experiments Eighth Edition, vol. 2. 2012.

[16]. S. Kumar, H. Meena, S. Chakraborty, and B. C. Meikap, "International Journal of Mining Science and Technology Application of response surface methodology (RSM) for optimization of leaching parameters for ash reduction from low-grade coal," Int. J. Min. Sci. Technol., vol. 28, no. 4, pp. 621–629, 2018.

[17]. K. T. Chiang, C. C. Chou, and N. M. Liu, "Application of response surface methodology in describing the thermal performances of a pin-fin heat sink," Int. J. Therm. Sci., vol. 48, no. 6, pp. 1196–1205, 2009.